GJB5 association with BRAF mutation and survival in cutaneous malignant melanoma

M Scatolini 1, A Patel 2, E Grosso 1, M Mello-Grand 3, P Ostano 3, R Coppo 4 5, M Vitiello 6, T Venesio 7, A Zaccagna 7, A Pisacane 7, I Sarotto 7, D Taverna 4, L Poliseno 6, D Bergamaschi 2, G Chiorino 3

1Molecular Oncology Laboratory, Fondazione Edo ed Elvo Tempia, 13875, Ponderano (BI), Italy.

2Centre for Cell Biology and Cutaneous Research, Blizard Institute, Barts and The London School of Medicine and Dentistry, Queen Mary University of London, London, E1 2AT, UK.

3Cancer Genomics Laboratory, Fondazione Edo ed Elvo Tempia, 13900, Biella, Italy.

4Molecular Biotechnology Centre, 10126, Torino, Italy.

5Department of Clinical Bio-Resource Research and Development, Graduate School of Medicine, Kyoto University, Kyoto, Japan.

6Oncogenomics Unit, Core Research Laboratory, Istituto Toscano Tumori, Institute of Clinical Physiology, CNR, 56124, Pisa, Italy.

7Pathology and Dermosurgery Units, Candiolo Cancer Institute (FPO-IRCCS), 10060, Candiolo, Turin, Italy.

Summary

Background

Gap-junctional intercellular communication is crucial for epidermal cellular homeostasis. Inability to establish melanocyte–keratinocyte contact and loss of the intercellular junction's integrity may contribute to melanoma development. Connexins, laminins and desmocollins have been implicated in the control of melanoma growth, where their reduced expression has been reported in metastatic lesions.

Objectives

The aim of this study was to investigate connexin 31·1 (GJB5) expression and identify any association with BRAF mutational status, prognosis of patients with melanoma and mitogen-activated protein kinase (MAPK) inhibitor (MAPKi) treatment.

Methods

GJB5 expression was measured at RNA and protein level in melanoma clinical samples and established cell lines treated (or not) with BRAF and MEK inhibitors (MEKi), as well as in cell lines which developed MAPKi resistance. Findings were further validated and confirmed by analysis of independent datasets.

Results

Our analysis reveals significant downregulation of GJB5 expression in metastatic melanoma lesions compared with primary ones and in BRAF-mutated vs. BRAF-wildtype (BRAFWT) melanomas. Likewise, GJB5 expression is significantly lower in BRAFV600E compared with BRAFWT cell lines and increases on MAPKi treatment. MAPKi-resistant melanoma cells display a similar expression pattern compared with BRAFWT cells, with increased GJB5 expression associated with morphological changes. Enhancement of BRAFV600E expression in BRAFWT melanoma cells significantly upregulates miR-335-5p expression with consequent downregulation of GJB5, one of its targets. Furthermore, overexpression of miR-335-5p in two BRAFWT cell lines confirms specific GJB5 protein downregulation. Reverse transcriptase quantitative polymerase chain reaction analysis also revealed upregulation of miR-335 in BRAFV600E melanoma cells, which is significantly downregulated in cells resistant to MEKi. Our data were further validated using the TCGA_SKCM dataset, where BRAF mutations associate with increased miR-335 expression and inversely correlate with GJB5 expression. In clinical samples, GJB5 underexpression is also associated with patient overall worse survival, especially at early stages.

Conclusions

Cutaneous melanoma originates by uncontrolled growth of melanocytes. Usually, each melanocyte forms contacts with about 30 keratinocytes within the basal and suprabasal layers forming the epidermal–melanin unit,1 and the connexin compatibilities of the two cell types render them capable of hetero-cellular gap-junctional intercellular communication (GJIC).2 GJIC is important for the maintenance of cellular homeostasis, regulation of proliferation, differentiation and apoptosis. Loss of the ability to form hetero-cellular contacts and exhibit GJIC to keratinocytes may contribute to melanoma growth within the epidermis.1 Gap junctions were first implicated in tumorigenesis nearly 50 years ago.3 In several studies GJIC resulted compromised in cancer cell lines, due to the downregulation or even absence of connexins.4–6 Knockout mice for connexin 32 (Cx32) were shown to be prone to developing chemical- and radiation-induced tumours, supporting the thesis that connexins have tumour-suppressor properties.7, 8 In agreement with those findings, connexin 26 or 43 (Cx26 or Cx43) ectopic expression in tumour cells causes a reduction of tumorigenic behaviours.9 More recently, connexins have also been linked with tumour growth progression at late stages of the disease,10 and defined as conditional tumour suppressors. Finally, a recent report revealed an important role for Cx43 in controlling melanoma growth, death and metastasis, emphasizing the potential use of compounds that selectively enhance connexin expression in future chemotherapy/immunotherapy protocols.11 An even more recent review suggests that Cx46 could

also have an important role in melanoma growth and early stages of metastasis, encouraging the scientific community to further investigate the role of connexins in melanoma progression and survival.12

In a previous work, we performed whole-genome expression profiling of 57 melanocytic lesions and noticed a strong enrichment of collagens, laminins, desmocollins and connexins within the genes with reduced expression in melanoma metastases (MTS).13 In particular, both GJB5 (gap-junction protein, Beta 5, Cx31·1) and GJB2 (gap-junction protein, Beta 2, Cx26) were significantly downregulated in metastases compared with vertical growth phase melanomas (VGPM). GJB2 expression in melanoma tissue has been shown to promote a metastatic cell phenotype and enhance the establishment of new tumour niches through cell-to-cell communication with the surrounding tissue.12 Regarding GJB5, a recent report has shown that it acts as a key regulator of migration and invasion in lung cancer cells,14 although no specific study on GJB5 in melanoma has been published so far. We therefore further explored the role of GJB5 in melanoma using published melanoma expression datasets, also focusing on its possible relationship with BRAF mutation. Then, exploiting a cohort of fresh and fixed melanoma tissues as well as established melanoma cell lines, we characterized GJB5 gene and protein expression in BRAF-mutated with respect to BRAF and NRAS wildtype melanomas, and in sensitive and resistant melanoma cells on treatment with mitogen activated protein kinase (MAPK) inhibitors (MAPKi). Measurement of miR-335 suggested its involvement in the regulation of GJB5 expression in melanoma cells. Lastly, our work revealed a strong association between GJB5 and patient prognosis.

Materials and methods

Tissue samples

GJB5 mRNA expression was analysed in 37 samples (14 common melanocytic naevi, 18 primary melanomas and five melanoma metastases, shown in Table 1) from a cohort of frozen lesions previously profiled by whole-genome microarrays.13 Naevi and primary melanomas were also genotyped for BRAF and NRAS mutation, starting from formalin-fixed paraffin-embedded (FFPE) tissue sections. An independent cohort of 25 FFPE samples (19 primary melanomas and six naevi) was also collected and genotyped to validate microarray results for GJB5 expression at the protein level by immunohistochemistry (IHC). All tissue samples were collected at the Candiolo Cancer Institute (FPO-IRCCS) as previously described,13 in agreement with the research rules of its Ethical Committee on human experimentation. Appropriate written informed consent was collected from all individuals included in the analysis.

Melanoma cell lines

The following melanoma cell lines were used: five BRAFWT (Mel 505, HBL, LM1, CHL-1 and C8161), five BRAFV600E (A375M, WM1158, WM278, WM793 and WM164), two NRASQ61mt (LM6 and WM1361), four vemurafenib (PLX4032)-resistant (A375M-PLX, WM1158-PLX, WM278-PLX and WM793-PLX) and one trametinib-resistant (A375M-TR). Mel 505 cells were grown in RPMI medium supplemented with 10% fetal bovine serum (FBS), 1% glutamine and 0·5% nonessential amino acid. HBL cells were cultured in DMEM medium supplemented with 10% FBS and 1% glutamine. All the other melanoma cell lines were grown in RPMI medium supplemented with 10% FBS and 1%

glutamine and for C8161 20 mmol L–1 Hepes and 0·1% gentamicin sulphate were also added. Vemurafenib- and trametinib-resistant melanoma cell lines were generated in the lab by chronic exposure with PLX4032 or trametinib. Each parental cell line was independently treated with increasing concentrations of PLX4032 up to 3 μmol L–1 or trametinib up to 50 nmol L–1 in a stepwise manner to generate an isogenic-resistant subline. Cells with the ability to grow in 3 μmol L–1 of PLX4032 or 50 nmol L–1 trametinib were obtained ~3 months after the initial drug exposure. Resistance to PLX4032 or trametinib was confirmed by lack of Phospho-MEK or Phospho-ERK inhibition on MAPKi exposure.15 All resistant cells were maintained in RPMI medium supplemented with 10% FBS, 1% glutamine and 3 μmol L–1 PLX4032 or 50 nmol L–1 trametinib, respectively.

DNA mutation analysis

Fresh and fixed tissues derived from each lesion were macro-dissected and DNA was isolated by using QIAamp DNA micro Kit (Qiagen). BRAF exon 15 and NRAS exons 2 and 3 were amplified by polymerase chain reaction (PCR) using primers and conditions as previously reported.16 NRAS exons 2 and 3 were amplified using the following primers: exon 2, forward 5'-ATGACTGAGTACAAACTGGT and reverse 5'-CTCTATGGTGGGATCATATT; exon 3, forward 5'-TCTTACAGAAAACAAGTG and reverse 5'-GTAGAGGTTAATATCCGCAA. PCR conditions for NRAS exons 2 and 3 were the same: initial denaturation at 95 °C for 5 min, 36 cycles at 95 °C for 30 s, at 52 °C for 30 s, at 72 °C for 30 s, followed by final elongation at 72 °C for 7 min. PCR products were purified by ExoSAP-IT (USB Corporation, Cleveland, OH, USA) and sequenced using Big Dye Terminator V3·1 Cycle Sequencing Kit on AB3500dx DNA Analyzer (Life Technologies). Sequence analysis was performed by Variant Reporter (Life Technologies). The percentage of mutated alleles for each BRAFV600E sample was established by means of pyrosequencing.15 Samples were divided into three groups: BRAFWT, BRAF+ and BRAF++ according to percentages of mutated alleles (none, 50–75%, > 75%).

Gene expression datasets

Gene expression profiles of our cohort are available on Gene Expression Omnibus public database (GSE12391).13 The following external datasets were used in the analyses: GSE8401,17 TCGA_SKCM (http://cancergenome.nih.gov/), GSE3189,18 GSE19234,19 GSE65904,20 GSE4651721 and the Leeds Melanoma Cohort (LMC) currently held within the European Genome–Phenome Archive at the European Bioinformatics Institute (accession number EGAS00000000029).

Gene selection and annotation

To compare class expression patterns between BRAF-mutated and BRAF/NRAS wildtype samples, moderated t-test and empirical Bayes statistics were applied using the R package limma (Linear Models for Microarray Data).22 Transcripts with significant modulation (B > 2) for empirical Bayes statistics were considered further.

One-way anova with Benjamini–Hochberg correction for multiple testing23 was applied to compare gene expression in BRAFWT, BRAF+ and BRAF++ classes. Transcripts with significant P-value (< 0·01), increasing or decreasing expression trends and absolute difference > 0·7 between BRAFWT and BRAF++ were considered further.

GSEA software24 was used to perform gene-set enrichment analysis. The NCBI database (http://www.ncbi.nlm.nih.gov/) and UCSC Genome Bioinformatics websites were used (http://genome.ucsc.edu/) to retrieve functional information on selected genes.

Taqman advance miRNA assay

After RNA extraction, 10 ng were used to perform a reverse-transcription reaction using TaqManTM Advanced miRNA cDNA Synthesis Kit (#A28007), according to the manufacturer's instructions. Quantitative PCR reactions were performed with the cDNA using TaqManTM Fast Advanced Master Mix (#4444965) and TaqManTM Advance miRNA assays from Thermo Fisher Scientific (hsa-miR-335-5p, sequence: UCAAGAGCAAUAACGAAAAAUGU, assay ID: 478324_mir; hsa-miR-25-3p, sequence: CAUUGCACUUGUCUCGGUCUGA, assay ID: 477994_mir). All reactions were performed in triplicate on a 96-well plate on a StepOnePlusTM real-time PCR machine (Thermo Fisher Scientific) and miR-25-3p, a recommended endogenous control, was used to normalize the expression of all miRNA assays.25 The cycle threshold (Ct) values of target miRNAs were normalized to the Ct value for miR-25-3p. The miRNA samples were analysed using the 2–ΔΔCT method.

Immunohistochemistry

Histological sections (4 μm) were mounted on silanized slides and allowed to dry for 1 h at room temperature, followed by 1-h incubation in an oven at 60 °C. Immunohistochemical staining (IHC) for GJB5 was performed according to our standard routine protocol using the Envision Flex (DAKO, Glostrup, Denmark). Fixed sections were retrieved in citrate buffer at pH 6·0 in Target Retrieval Solution (DAKO) in a high-pressure cooker and incubated with polyclonal rabbit antibody anti-human GJB5 (1 : 50, #67290, Abcam, Cambridge, UK) for 60 min at room temperature. Negative control slides were incubated with the antibody diluent alone and no primary antibody under equivalent conditions. The final reaction was visualized using 3,3'-diaminobenzidine (DAB) in a buffer/hydrogen peroxide solution for 10 min. Finally, sections were counterstained with Harris's haematoxylin, dehydrated and mounted in DPX. Immuno-positive cells were determined semi-quantitatively in a percentage of the total tumour cell fraction. GJB5 expression has been calculated as cytoplasmic intensity score (1-2-3).

Western blot analysis

Cells were seeded in six-well plates and the day after treated with DMSO, 3 μmol L–1 PLX4032 or 50 nmol L–1 trametinib (GSK1120212) (Selleck Chemicals, Houston, TX, USA). After 24–48 h, the cells were harvested and lysed with RIPA lysis buffer. An equal amount of protein lysates was resuspended in 10X NuPage reducing agent (Invitrogen #NP0009) and 4X NuPage lithium dodecyl sulfate sample buffer (Invitrogen #NP0007). Samples were mixed and heated at 70 °C for 10 min. Protein samples were resolved using Bis-Tris gels. Upon completion of protein transfer, the membrane was washed, blocked for 1 h with 1% bovine serum albumin (BSA, Sigma) in phosphate-buffered saline (PBS) and incubated with anti-GJB5 antibody (1 : 500, sc-515690, Santa Cruz Biotechnology, Santa Cruz, CA, USA) and anti-glyceraldehyde-3-phosphate dehydrogenase (GAPDH) (1 : 2500, #G9545, Sigma-Aldrich, St Louis, MO, USA) in PBS with 1% BSA at 4 °C overnight. After three washes (10-min each) in PBS-Tween 0·1%, the secondary antibody incubation was performed using a peroxidase-conjugated antimouse (1 : 5000 DAKO) or antirabbit (1 : 10 000 DAKO) antibody in PBS-Tween 0·1% with 1% BSA

for 45 min. After three washes in PBS-Tween 0·1%, a bound secondary antibody was detected by enhanced chemiluminescence with ECL (GE Healthcare) according to the manufacturer's protocol.

Immunofluorescence

Cells were seeded in 24-well plates onto coverslips, treated with DMSO, 3 µmol L–1 PLX4032 or 50 nmol L–1 trametinib for 24–48 h and fixed in 4% formaldehyde. Once washed in PBS, cell membranes were permeabilized in 0·3% Triton X-100 for 2 min at room temperature; coverslips were then washed twice with PBS for 10 min to remove any residual detergent. Cells were incubated with 5% goat serum/PBS for 30 min followed by incubation with anti-GJB5 antibody diluted in 5% goat serum/PBS overnight at 4 °C. Cells were washed three times for 10 min in PBS and incubated with the appropriate fluorophore-coupled secondary antibody (1 : 500) for 1 h at room temperature in the dark. Cells were washed twice for 10 min in PBS then incubated with 4',6-diamidino-2-phenylindole (DAPI) for 10 min followed by two washes in PBS for 10 min. Coverslips were mounted onto a glass slide using Vectashield Mounting Medium and imaged with a Zeiss upright 710 confocal microscope.

GJB5 expression regulation

Overexpression

Cells seeded on six-well plates were transiently transfected with a GJB5 untagged expression plasmid (#SC123764) or with an empty vector plasmid using Polyplus jetPRIME transfection reagent (Polyplus-transfection® SA). One µg of plasmid DNA diluted in Polyplus jetPRIME reagent was transfected in each well according to the manufacturer's protocol. Cells were harvested at 48 h and GJB5 expression was assessed by Western blotting.

siRNA

Cells seeded onto six-well plates were silenced using Polyplus jetPRIME transfection reagent (Polyplus-transfection® SA), according to the manufacturer's instructions. A pool of three small interfering RNA (siRNA) sequences (#SC-88186, Santa Cruz Biotechnology) were used to silence GJB5. Briefly, siRNA at a concentration of 50 nmol L–1 was incubated with Polyplus jetPRIME reagent in Penicillin/Streptomycin-free media. Control cells were either untreated or transfected with a scramble Si-RNA sequence. Cells were harvested at 48 h and GJB5 downregulation was assessed by Western blotting.

hsa-mir-335

After cell seeding onto six-well plates, a MISSION miRNA mimic for miR-335 (#HMI0490, Sigma-Aldrich) and an unrelated miRNA control were introduced into the cells, according to the manufacturer's instructions. The miRNA mimic was incubated with Polyplus jetPRIME reagent at a concentration of 10 nmol L–1. Cells were harvested at 48 h and expression of GJB5 on miRNA mimics expression was assessed by Western blotting.

Statistical analysis

Student's t-test was applied to check statistical significance in two-class comparison using reverse-transcriptase quantitative polymerase chain reaction (RT-qPCR) data, using 0·05 as the cutoff for P-values. Kaplan–Meier analysis was performed using the survival package from R.

Results

GJB5 expression decreases with melanoma progression and is inversely correlated with BRAF mutation

GJB5 expression in the clinical samples we previously profiled (GSE12391 dataset)13 showed a strong decrease (moderated t-test, P-value < 0·0001) from primary (n = 23) to metastatic (n = 5) melanomas (Figure 1a). This finding was confirmed in other larger published datasets, such as GSE8401 (Figure 2a) and TCGA_SKCM (Figure 2b). In common naevi, GJB5 was more expressed than in primary melanomas, both in our (Figure 2c) and in other published datasets, such as GSE3189 (Figure 2d).

No lesion in our cohort was mutated in NRAS exons 2–3, while BRAF mutation in exon 15 was found in 60% of the samples. Within the group of genes with higher expression in mutated melanomas or with an increasing trend from wildtype melanomas to BRAF++, we identified Enhancer of Polycomb Homolog 1 (EPC1), SRY-Box 2 (SOX2) and Catenin Beta 1 (CTNNB1), all stem-cell markers (Figure 1b–d). Conversely, GSEA revealed that the downregulated transcripts were enriched in cadherins, serpins, laminins, connexins and genes that negatively regulate the formation of metastases (Figure 1e). Among them, the most significant was indeed GJB5. GJB5 showed a decreasing trend from BRAFWT to BRAF++ melanomas (Figure 1f), with a lower expression in BRAF-mutated than in BRAFWT lesions (F-statistics, P-value = 0·0063). Analysis of TCGA_SKCM metastatic samples confirmed this trend (Figure 2e) (t-test, P-value = 0·023). Because about 80% of naevi are positive for the BRAF mutation,26 we evaluated the expression of GJB5 within our cohort of common naevi, observing a lower, although not significantly, expression in BRAF-mutated vs. BRAFWT naevi (logFC –0·7, t-test, P-value = 0·3).

An independent cohort of 25 fixed lesions (19 primary melanomas and six naevi) was stained for GJB5 expression and genotyped for BRAF and NRAS. In agreement with microarray data, lower GJB5 expression was confirmed in BRAFV600 compared with BRAFWT melanomas (Figure 3a, b) and common melanocytic naevi (Figure 3c, d).

GJB5 endogenous protein level was also analysed by Western blotting on several established melanoma cell lines. We report GJB5 downregulation in cell lines derived from metastatic lesions (A375M, C8161, WM1158, WM164, WM1361) compared with cell lines derived from primary melanomas (LM1, LM6, Mel 505). In the same panel of cell lines, connexin 26 (GJB2) displayed a more heterogeneous expression pattern (Figure 3e). Moreover, GJB5 protein expression was mainly detected in BRAFWT cell lines when compared with BRAFV600E melanoma cells (Figure 3f), supporting previous results obtained on clinical samples. Overexpression of GJB5 in BRAFV600E A375M cells did not affect the endogenous expression of other connexins (GJA1 and GJB1) (Figure 3g). To further

confirm this, GJA1, GJB1 and GJB2 expression did not compensate for GJB5 loss nor decrease when endogenous levels of GJB5 were downregulated by siRNA interference in two BRAFWT melanoma cell lines (Figure 3h).

GJB5 expression is restored on treatment of BRAFV600E melanoma cells with BRAF and MEK inhibitors and is regulated by miR-335-5p

To establish a link between the mutational status of BRAF and absence or downregulation of GJB5 expression, we investigated the effect of BRAF and MEK inhibition on GJB5 protein expression by exposing BRAFV600E melanoma cell lines to vemurafenib and/or trametinib.

Specific inhibition of BRAF with vemurafenib for 24 h produced an upregulation of GJB5 protein expression (Figure 4a, b) in BRAFV600E-mutated WM1158, A375M, WM793 and WM278 melanoma cells. Likewise, MEK inhibition with trametinib caused an increase of GJB5 levels in WM278, WM793 and A375M melanoma cells (Figure 4c–e), although the combined treatment (vemurafenib plus trametinib) did not result in a further increase (Figure 4c). We also observed that GJB5 was more expressed in vemurafenib-resistant cells (Figure 4a, b) as well as in trametinib-resistant ones (Figure 4d, e) compared with their parental cell lines, although upregulation in trametinib-resistant cells was also linked with a significant cytoskeleton dysregulation not observed in the vemurafenib-resistant cells (Figure 4e).

To further investigate how MAPK signalling could affect GJB5 expression, we transiently enhanced BRAFV600E expression in BRAFWT CHL-1 melanoma cells, which resulted in activation of phosphorylated MEK and ERK (Figure 4f). Upon transient expression of BRAFV600E, the expression of the only experimentally found microRNA that targets GJB5 (as reported in http://mirtarbase.cuhk.edu.cn/), namely miR-335-5p, significantly increased (Figure 4g), and was associated with GJB5 downregulation (Figure 4f). RT-qPCR analysis further confirmed miR-335-5p upregulation in BRAFV600E melanoma cell lines, which was reduced on development of MAPKi resistance, more significantly with MEK inhibitor (MEKi) resistance (Figure 4h). Likewise, transient overexpression of miR-335 mimics was able to reduce endogenous expression of GJB5 in two different BRAFWT melanoma cell lines without affecting the expression of GJB2 (Figure 4i).

Validation in TCGA_SKCM samples (n = 353) revealed a statistically significant tendency towards mutual exclusivity between mutated BRAF and GJB5 overexpression, co-occurrence of mutated BRAF and miR-335-5p gain, as well as a tendency towards mutual exclusivity between overexpressed GJB5 and miR-335-5p gain (Figure 4j, lower panel). miR-335-5p expression in BRAF-mutated (n = 114) was higher than in BRAFWT (n = 120) cutaneous melanomas (t-test, P-value = 0·06) (Figure 4j, upper panel).

GJB5 expression and survival of patients with melanoma

To evaluate whether the expression of GJB5 could have a prognostic value, we looked for any association between GJB5 mRNA level and patient survival (10 years of follow-up data) in our cohort of fresh melanoma tissues. Kaplan–Meier analysis revealed that patients with higher GJB5 expression

had a better prognosis compared with patients with lower GJB5 (P = 0·00148) (Figure 5a). Interestingly, all nine patients who died from melanoma were among the top 13 samples with lower GJB5 expression. The same analysis was repeated in four other datasets with available follow-up information (Figure 5b–e) and a positive association with better prognosis was confirmed, especially for the GSE46517 dataset (log-rank test P-value = 0·000009) and for the LMC which contains early stages only and is the largest one including more than 700 patients (log-rank test P-value = 0·00115).

Discussion

The data in the literature show the involvement of gap junctions in tumour progression and in particular their role as tumour suppressors.4–6 27 Lack of connexins was associated with development of chemical- and radiation-induced tumours,7, 8 while reintroduction of connexins was shown to decrease tumorigenic behaviours.9 Recently, Tittarelli and coworkers identified connexin 43 (Cx43) as an important key player in melanoma development and suggested the use of compounds that selectively enhance connexin expression for melanoma therapy.12 For example, all-trans retinoic acid (ATRA), an analogue of vitamin A, is currently being studied extensively for its potential as a therapeutic and chemopreventive agent. The antitumour effects of ATRA in various types of cancers are associated with its ability to restore gap-junction function of otherwise gap-junctional communication-impaired tumour cells.28, 29

US Food and Drug Administration approval of vemurafenib as the first BRAF inhibitor (BRAFi) in 2011 represented a milestone in melanoma therapy, and other similar compounds were successively developed and approved. However, as resistance to anti-BRAF therapy inevitably occurs, being able to characterize a BRAF signature in melanomas and find new potential druggable targets implicated in melanomagenesis/progression represent the major challenges at present of potentiating and prolonging anti-BRAF therapies.

We analysed the BRAF-associated transcriptome in a cohort of fresh melanocytic lesions13 and identified a signature characterized by the upregulation of metastatic processes and stem-cell markers, highlighting overlapping signalling networks that regulate both stem-cell migration and malignant melanoma dissemination.30–32 We also reported the downregulation of genes that negatively control the formation of metastases, including cadherins, serpins, laminins and connexins. Among them, GJB5 showed a significant lower expression in melanoma metastases compared with primary melanomas and in BRAF-mutated compared with wildtype lesions. Indeed, those results were confirmed in external published datasets. The inverse correlation between the presence of BRAF mutation and GJB5 expression was validated at the protein level by IHC, using an independent cohort of fixed primary melanomas as well as common melanocytic naevi. Interestingly, the protein was almost undetectable in BRAF-mutated cell lines, and it was re-expressed on treatment with BRAFi and MEKi, although with a different localization pattern.

Our results suggest a dependence of GJB5 expression on aberrant BRAF signalling, with mutant BRAF exerting inhibition and treatment targeting BRAF being able to restore its expression. In melanoma cell lines that developed MAPKi resistance on chronic exposure to vemurafenib or trametinib, GJB5 was

expressed, showing a similar pattern to BRAFWT ones. Even if MAPK signalling plays an important role in acquired resistance to BRAFi, probably in this context its role is not mainly responsible.32–34 PI3K–AKT,35 EGFR–SFK–STAT336 or other pathways involved in resistance mechanisms could have a role in explaining why GJB5 is re-expressed at basal levels such as in BRAFi-resistant cells or at high levels, such as in MEKi-resistant cells. For instance, MAPKi-resistant melanoma cells often display morphological changes and overall increased plasticity probably driven by cytoskeleton reorganization.15, 37

Expression of BRAF mutation in melanoma represents a negative prognostic factor.37–42 Here we have shown that induction of BRAFV600E in BRAFWT melanoma cells not only activated MAPK signalling but also upregulated miR-335-5p expression.43, 44 Measurement by RT-qPCR confirmed upregulation of miR-335-5p in BRAFV600E melanoma cell lines, which was significantly downregulated when cells became resistant to MEKi. To further confirm this, transduction of miR-335 in BRAFWT melanoma cells can specifically downregulate GJB5 protein expression, providing a novel mechanism of control of gap-junction integrity by BRAF via a microRNA (Figure 4k). This functional model has been further confirmed by an independent study (TCGA_SKCM dataset), where a correlation between increased miR-335-5p expression in BRAF-mutated melanoma samples and GJB5 downregulation was identified.

Previous studies have already shown that downregulation of connexins may enhance melanoma capability of developing metastases.45 Indeed, GJA1 is included into the prognostic genetic signature for cutaneous melanoma metastatic risk developed by Gerami and colleagues.46 Here we found that GJB5 expression was not only reduced in melanoma metastases but was also inversely associated with overall survival in our cohort (Figure 5a). This result was confirmed in two larger independent cohorts including 82 (Figure 5d) and 703 (Figure 5e) patients, respectively, and, to a lesser extent, in two other smaller cohorts (Figure 5b, c). All the datasets provided more than 10 years of follow-up information and the LMC did not contain any metastatic sample, thus strengthening the prognostic role of GJB5. Although information about patient treatment was not always available, any lower association could be linked with the advent of BRAFi and MEKi that have contributed in recent years to increased survival in advanced-stage mutated melanomas.

In summary, we identified a significant association between melanoma metastases/BRAF mutation and low GJB5 expression in fresh and fixed melanoma lesions, both at mRNA and protein levels. Analyses on melanoma cell lines confirmed a direct link between BRAF mutation and GJB5 expression via miR-335-5p, showing that GJB5 is restored in BRAFV600E cell lines on treatment with BRAFi and MEKi. Finally, overall survival analysis indicated an association between GJB5 expression and favourable outcome, supporting a prognostic role for GJB5 in cutaneous melanoma.

Acknowledgments

Human melanoma cell lines WM793, WM278, WM1158, WM164 and WM1361 were a gift from Prof. Meenhard Herlyn (Wistar Institute, Philadelphia, PA, USA). LM1 and LM6 were generously provided by Dr Monica Rodolfo (Fondazione IRCCS Istituto Nazionale Tumori, Milan, Italy). C8161 cells were a gift from Prof. M.J.C. Hendrix (Children's Memorial Research Center, Chicago, IL, USA). Mel 505 were provided by Dr Tim Crook (Southend University, Essex, UK). A375M were donated by Prof. John F.

Marshall (Barts Cancer Institute, QMUL, London, UK). HBL were provided by Prof. Jiri Vachtenheim (University Hospital Prague, Czech Republic). The results of this publication are based (partly) on data generated by the University of Leeds in connection with the project 'The Leeds Melanoma Cohort'; otherwise known as Melanoma Follow-up and Case–Control Family Study (REC reference number 01/03/057). These data are currently held within the European Genome–Phenome Archive at the European Bioinformatics Institute (accession number EGAS00000000029). The generation of these data were funded by Cancer Research UK (award refs C588/A19167, C8216/A6129 and C588/A10721) and with the support of the National Institutes of Health (award ref. CA83115) and the European Commission Horizon 2020 Research and Innovation Programme (ref. no. 641458).

Author Contribution

Maria Scatolini: Conceptualization (equal); Data curation (lead); Formal analysis (equal); Investigation (lead); Methodology (lead); Validation (equal); Visualization (equal); Writing-original draft (supporting); Writing-review & editing (supporting). Ankit Patel: Data curation (lead); Formal analysis (equal); Investigation (lead); Methodology (lead); Validation (equal); Visualization (equal); Writing-original draft (supporting); Writing-review & editing (supporting). Enrico Grosso: Data curation (equal); Formal analysis (equal); Investigation (equal). Maurizia Mello Grand: Data curation (equal); Formal analysis (equal); Investigation (equal). Paola Ostano: Data curation (equal); Formal analysis (equal); Investigation (equal). Roberto Coppo: Investigation (supporting); Methodology (supporting); Software (equal). Mariana Vitiello: Data curation (supporting); Formal analysis (supporting). Tiziana Venesio: Data curation (equal); Resources (equal). Alessandro Zaccagna: Data curation (equal); Formal analysis (equal). Alberto Pisacane: Data curation (equal); Formal analysis (equal). Ivana Sarotto: Data curation (equal); Formal analysis (equal). Daniela Taverna: Conceptualization (supporting). Laura Poliseno: Conceptualization (supporting); Data curation (supporting); Formal analysis (supporting). Giovanna Chiorino: Conceptualization (lead); Data curation (equal); Formal analysis (lead); Funding acquisition (lead); Investigation (lead); Methodology (equal); Resources (equal); Software (equal); Supervision (lead); Validation (lead); Visualization (lead); Writing-original draft (lead); Writing-review & editing (lead). Daniele Bergamaschi: Conceptualization (lead); Data curation (lead); Formal analysis (lead); Funding acquisition (supporting); Investigation (lead); Methodology (lead); Supervision (lead); Validation (lead); Visualization (lead); Writing-original draft (lead); Writing-review & editing (lead).

References

1 Haass NK, Smalley KS, Li L et al. Adhesion, migration and commu- nication in melanocytes and melanoma. Pigment Cell Res 2005; 18:150–9.

2 Hsu MY, Meier FE, Nesbit M et al. E-cadherin expression in mela- noma cells restores keratinocyte-mediated growth control and down-regulates expression of invasion-related adhesion receptors. Am J Pathol 2000; 156:1515–25.

3 Loewenstein WR. Permeability of membrane junctions. Ann N Y Acad Sci 1966; 137:441–72.

4 Krutovskikh V, Mazzoleni G, Mironov N et al. Altered homologous and heterologous gap-junctional intercellular communication in primary human liver tumors associated with aberrant protein

localization but not gene mutation of connexin 32. Int J Cancer

1994; 56:87–94.

5 Mesnil M, Crespin S, Avanzo JL et al. Defective gap junctional intercellular communication in the carcinogenic process. Biochim Biophys Acta 2005; 1719:125–45.

6 Cronier L, Crespin S, Strale PO et al. Gap junctions and cancer: new functions for an old story. Antioxid Redox Signal 2009; 11:323–38.

7 Temme A, Buchmann A, Gabriel HD et al. High incidence of spon- taneous and chemically induced liver tumors in mice deficient for connexin32. Curr Biol 1997; 7:713–16.

8 King TJ, Lampe PD. Mice deficient for the gap junction protein connexin32 exhibit increased radiation-induced tumorigenesis associated with elevated mitogen-activated protein kinase (p44/Erk1, p42/Erk2) activation. Carcinogenesis 2004; 25:669–80.

9 McLachlan E, Shao Q, Wang HL et al. Connexins act as tumor sup- pressors in three-dimensional mammary cell organoids by regulat- ing differentiation and angiogenesis. Cancer Res 2006; 66:9886–94.

10 Naus CC, Laird DW. Implications and challenges of connexin con- nections to cancer. Nat Rev Cancer 2010; 10:435–41.

11 Tittarelli A, Guerrero I, Tempio F et al. Overexpression of connexin

43 reduces melanoma proliferative and metastatic capacity. Br J Cancer 2016; 115:e14.

12 Orellana VP, Tittarelli A, Retamal MA. Connexins in melanoma: potential role of Cx46 in its aggressiveness. Pigment Cell Melanoma Res 2021; 34:853–68.

13 Scatolini M, Grand MM, Grosso E et al. Altered molecular pathways in melanocytic lesions. Int J Cancer 2010; 126:1869–81.

14 Zhang D, Chen C, Li Y et al. Cx31.1 acts as a tumour suppressor in non-small cell lung cancer (NSCLC) cell lines through inhibi- tion of cell proliferation and metastasis. J Cell Mol Med 2012; 16:1047–59.

15 Patel A, Garcia LF, Mannella V et al. Targeting p63 upregulation abrogates resistance to MAPK inhibitors in melanoma. Cancer Res 2020; 80:2676–88.

16 Venesio T, Chiorino G, Balsamo A et al. In melanocytic lesions the fraction of BRAFV600E alleles is associated with sun exposure but unrelated to ERK phosphorylation. Mod Patho 2008; 21:716–26.

17 Xu L, Shen SS, Hoshida Y et al. Gene expression changes in an ani- mal melanoma model correlate with aggressiveness of human mel- anoma metastases. Mol Cancer Res 2008; 6:760–9.

18 Talantov D, Mazumder A, Yu JX et al. Novel genes associated with malignant melanoma but not benign melanocytic lesions. Clin Can- cer Res 2005; 11:7234–42.

19 Bogunovic D, O'Neill DW, Belitskaya-Levy I et al. Immune profile and mitotic index of metastatic melanoma lesions enhance clinical staging in predicting patient survival. Proc Natl Acad Sci U S A 2009; 106:20429–34.

20 Cirenajwis H, Ekedahl H, Lauss M et al. Molecular stratification of metastatic melanoma using gene expression profiling: prediction of survival outcome and benefit from molecular targeted therapy. Oncotarget 2015; 6:12297–309.

21 Kabbarah O, Nogueira C, Feng B et al. Integrative genome compar- ison of primary and metastatic melanomas. PLoS One 2010; 5: e10770.

22 Ritchie ME, Phipson B, Wu D et al. limma powers differential expression analyses for RNA-sequencing and microarray studies. Nucleic Acids Res 2015; 43:e47.

23 Benjamini Y, Hochberg Y. Controlling the false discovery rate: a practical and powerful approach to multiple testing. J R Stat Soc Ser- ies B (Method) 1995; 57:289–300.

24 Subramanian A, Tamayo P, Mootha VK et al. Gene set enrichment analysis: a knowledge-based approach for interpreting genome-wide expression profiles. Proc Natl Acad Sci U S A 2005; 102:15545–50.

25 Das MK, Andreassen R, Haugen TB, Furu K. Identification of endogenous controls for use in miRNA quantification in human cancer cell lines. Cancer Genomics Proteomics 2016; 13:63–8.

26 Pollock PM, Harper UL, Hansen KS et al. High frequency of BRAF mutations in nevi. Nat Genet 2003; 33:19–20.

27 Aasen T, Leithe E, Graham SV et al. Connexins in cancer: bridging the gap to the clinic. Oncogene 2019; 38:4429–51.

28 Watanabe J, Nomata K, Noguchi M et al. All-trans retinoic acid enhances gap junctional intercellular communication among renal epithelial cells in vitro treated with renal carcinogens. Eur J Cancer 1999; 35:1003–8.

29 Wang J, Dai Y, Huang Y et al. All-trans retinoic acid restores gap junctional intercellular communication between oral cancer cells with upregulation of Cx32 and Cx43 expressions in vitro. Med Oral Patol Oral Cir Bucal 2013; 18:e569–77.

30 Christgen M, Geffers R, Ballmaier M et al. Down-regulation of the fetal stem cell factor SOX17 by H33342: a mechanism responsible for differential gene expression in breast cancer side population cells. J Biol Chem 2010; 285:6412–18.

31 Fong H, Hohenstein KA, Donovan PJ. Regulation of self-renewal and pluripotency by Sox2 in human embryonic stem cells. Stem Cells 2008; 26:1931–8.

32 Takahashi-Yanaga F, Kahn M. Targeting Wnt signaling: can we safely eradicate cancer stem cells? Clin Cancer Res 2010; 16:3153– 62.

33 Sosman JA, Kim KB, Schuchter L et al. Survival in BRAF V600- mutant advanced melanoma treated with vemurafenib. N Engl J Med 2012; 366:707–14.

34 Solit DB, Rosen N. Towards a unified model of RAF inhibitor resistance. Cancer Discov 2014; 4:27–30.

35 Villanueva J, Vultur A, Lee JT et al. Acquired resistance to BRAF inhibitors mediated by a RAF kinase switch in melanoma can be overcome by cotargeting MEK and IGF-1R/PI3K. Cancer Cell 2010; 18:683–95.

36 Prahallad A, Sun C, Huang S et al. Unresponsiveness of colon can- cer to BRAFV600E inhibition through feedback activation of EGFR. Nature 2012; 483:100–3.

37 Kim MH, Kim J, Hong H et al. Actin remodeling confers BRAF inhibitor resistance to melanoma cells through YAP/TAZ activa- tion. Embo J 2016; 35:462–78.

38 Long GV, Menzies AM, Nagrial AM et al. Prognostic and clinico- pathologic associations of oncogenic BRAF in metastatic mela- noma. J Clin Oncol 2011; 29:1239–46.

39 Safaee Ardekani G, Jafarnejad SM, Tan L et al. The prognostic value of BRAF mutation in colorectal cancer and melanoma: a systematic review and meta-analysis. PLoS One 2012; 7:e47054.

40 Moreau S, Saiag P, Aegerter P et al. Prognostic value of BRAFV600 mutations in melanoma patients after resection of metastatic lymph nodes. Ann Surg Oncol 2012; 19:4314–21.

41 Picard M, Pham Dang N, D'Incan M et al. Is BRAF a prognostic factor in stage III skin melanoma? A retrospective study of 72 patients after positive sentinel lymph node dissection. Br J Dermatol 2014; 171:108–14.

42 Barbour AP, Tang YH, Armour N et al. BRAF mutation status is an independent prognostic factor for resected stage IIIB and IIIC mel- anoma: implications for melanoma staging and adjuvant therapy. Eur J Cancer 2014; 50:2668–76.

43 Calderon JF, Retamal MA. Regulation of connexins expression levels by microRNAs, an update. Front Physiol 2016; 7:558.

44 Tavazoie SF, Alarcon C, Oskarsson T et al. Endogenous human microRNAs that suppress breast cancer metastasis. Nature 2008; 451:147–52.

45 Stoletov K, Strnadel J, Zardouzian E et al. Role of connexins in metastatic breast cancer and melanoma brain colonization. J Cell Sci 2013; 126:904–13.

46 Gerami P, Cook RW, Wilkinson J et al. Development of a prognos- tic genetic signature to predict the metastatic risk associated with cutaneous melanoma. Clin Cancer Res 2015; 21:175–83

Table 1 Patients characteristics of fresh frozen tissue samples used for gene expression profiling experiments and BRAF/NRAS sequencing. All samples were NRAS wildtype

Sample	Sex	Histotype	Site	$BRAF^{V600E}$	Stage
N31	M	Compound naevus	Sovra-gluteal	WT	CMN
N29	F	Compound naevus	Arm	WT	CMN
N32	M	Intradermal naevus	Shoulder	WT	CMN
N28	F	Junctional naevus	Pubis	WT	CMN
N25	F	Compound naevus	Breast	WT	CMN
N23	F	Intradermal naevus	Peri-umbilical	++	CMN
N27	F	Compound naevus	Hip	++	CMN
N35	F	Compound naevus	Leg	++	CMN
N26	M	Compound naevus	Back	++	CMN
N36	F	Intradermal naevus	Lumbar region	++	CMN
N4	F	Compound naevus	Thigh	+	CMN
M10a	M	Compound underlying naevus	Shoulder	+	CMN
N22a	M	Junctional naevus	Lumbar region	+	CMN
N22b	M	Compound naevus	Back	+	CMN
M3	M	CL II; 0·3 mm	Arm	WT	RGPM
M6	M	CL IV; 2·2 mm	Thigh	WT	VGPM
M23b	M	CL IV; 1·7 mm	Thigh	WT	VGPM
M42	M	CL V; 8·5 mm	Armpit	WT	VGPM
M40	M	CL IV; 1 mm	Chest	WT	VGPM
M1a	F	CL IV; 0·9 mm	Leg	WT	VGPM
M14	M	CL III; 0·65 mm	Thigh	++	VGPM
M18	M	CL IV; 9 mm	Back	++	VGPM
M13	F	CL III; 0·65 mm	Arm	++	VGPM
M12	F	CL II; 0·2 mm	Leg	++	RGPM
M20	M	CL II; 0·3 mm	Chest	++	RGPM
M24a	F	CL III; 0·7 mm	Back	+	VGPM
M21	F	CL II; 0·5 mm	Shoulder	+	RGPM
M35	M	CL IV; 9 mm	Back	+	VGPM
M37	M	CL V; 10 mm	Chest	+	VGPM
M11	M	CL IV; 0·3 mm	Shoulder	+	VGPM
M25	F	CL V; 6 mm	Leg	+	VGPM
M10b	M	CL II; 0·3 mm	Shoulder	+	RGPM
M30	F		Thigh		MTS
M38	F		Derma		MTS
M8	M		Node		MTS
M36	F		Node		MTS
M33	M		Back		MTS

CL, Clark level; CMN, common melanocytic naevus; MTS, metastatic; RGPM, radial growth phase melanoma; VGPM, vertical growth phase melanoma; WT, wildtype.

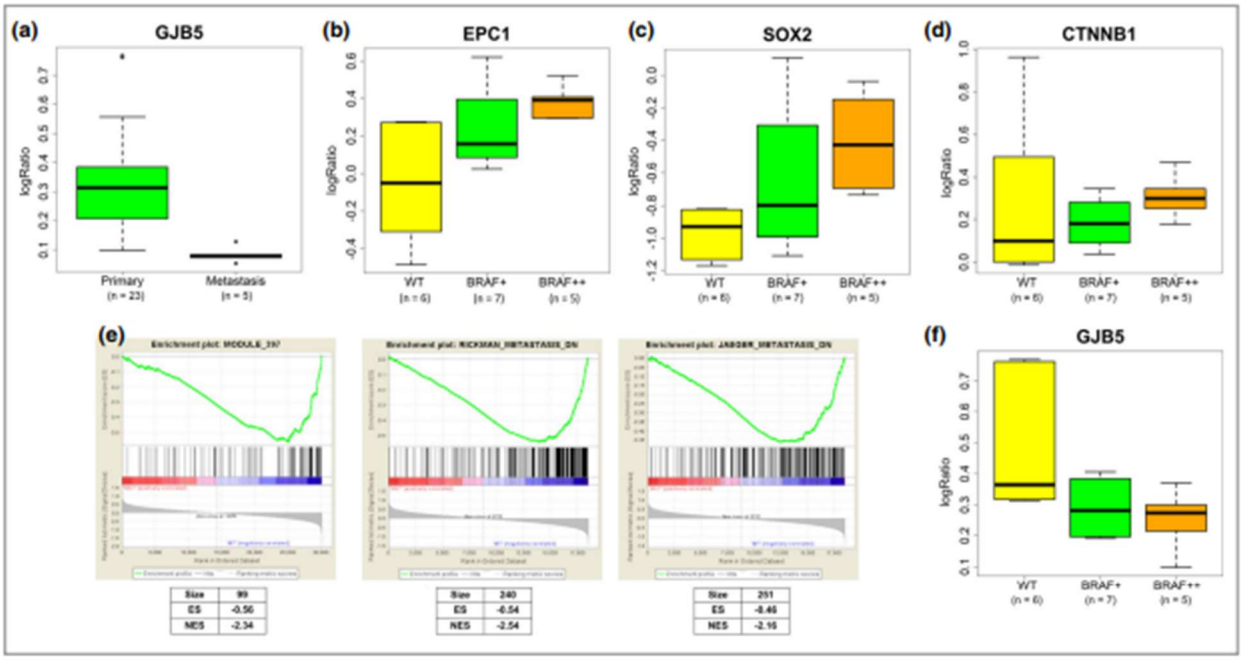

Figure 1 (a) GJB5 expression levels in melanoma samples. Boxplots showing GJB5 expression in primary (RGPM, VGPM) compared with melanoma metastases, derived from microarray data (moderated t-test, P-value < 0·0001). (b–d, f) Boxplots showing EPC1 (b), SOX2 (c), CTNNB1 (d) and GJB5 (f) expression in $BRAF^{WT}$, $BRAF^{V600+}$ and $BRAF^{V600++}$ in melanoma samples classes, derived from microarray data (F-statistics, P-value < 0·01). (e) Gene expression profiling data generated by microarray were analysed using gene-set enrichment analysis to extract biological knowledge. Module_297,[a] Rickman_metastasis_DN and Jaeger_metastasis_DN gene sets were highly significantly enriched (false discovery rate q-value < 0·005) within the genes downregulated in BRAF-mutated samples. [a]https://www.gsea-msigdb.org/gsea/msigdb/cards/module_297. RGPM, radial growth phase melanoma; VGPM, vertical growth phase melanoma; WT, wild-type.

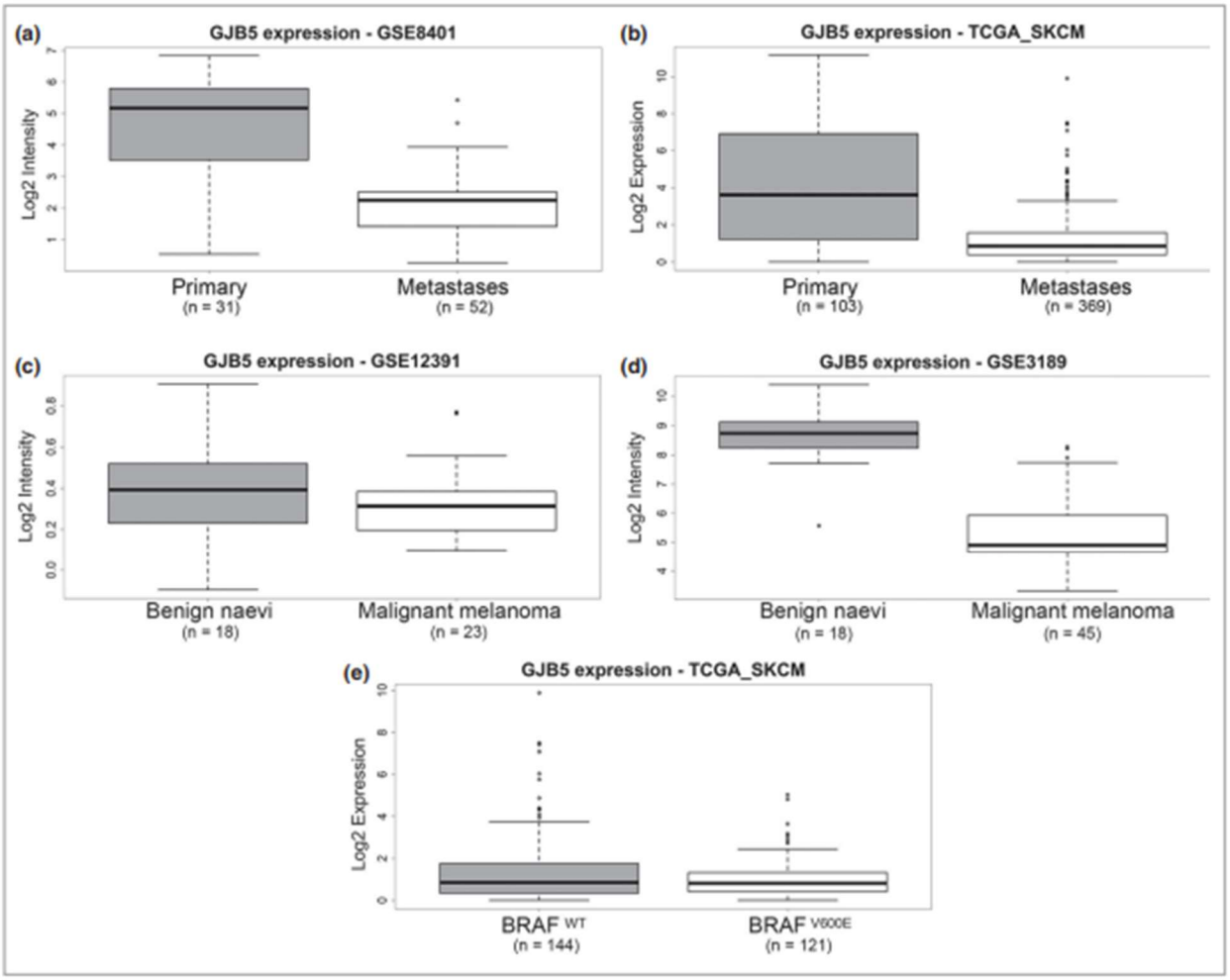

Figure 2 GJB5 expression in external datasets. (a, b) GJB5 expression in primary vs. metastatic melanomas from GSE8401 and TCGA_SKCM datasets (t-test, *P*-value < 0·001). (c, d) GJB5 expression profile in benign naevi and in malignant melanomas from GSE12391 and GSE3189 datasets (t-test, *P*-value < 0·001). (e) GJB5 expression in *BRAF*-mutated vs. *BRAF* wildtype metastatic melanomas from TCGA_SKCM (t-test, *P*-value = 0·05).

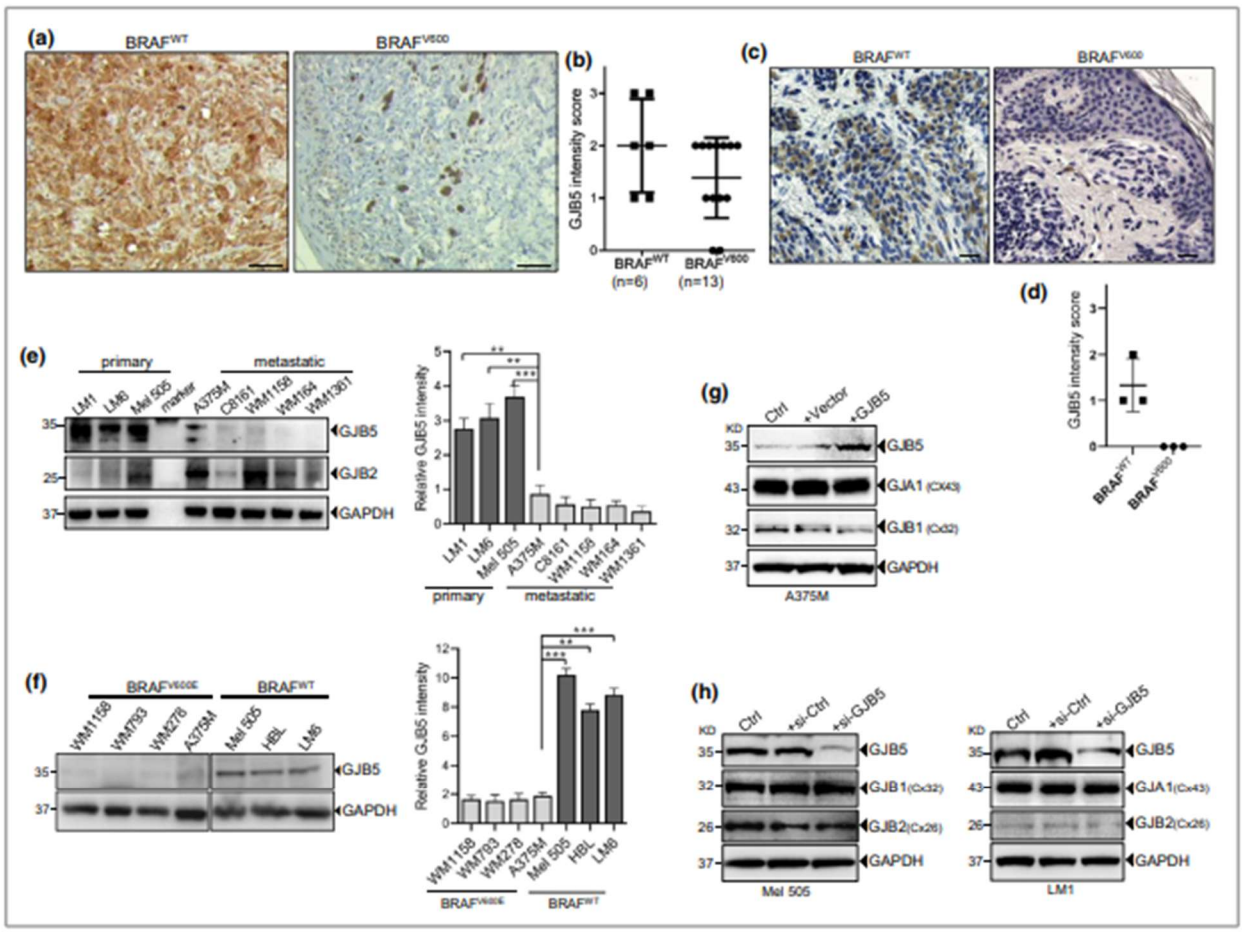

Figure 3 GJB5 expression in melanocytic lesions in relation to BRAF status and disease progression. (a) Immunohistochemical analysis of GJB5 staining in melanomas. GJB5 protein expression in $BRAF^{WT}$ (left panel) compared with $BRAF^{V600E}$ melanoma (right panel). (b) GJB5 intensity scores in the two classes of melanoma lesions. (c) Immunohistochemical analysis of GJB5 staining and (d) quantification of intensity scores in naevi with different BRAF mutational status. Black scale bars represent 100 μm. (e) Western blot analysis of GJB5 and GJB2 protein expression in cell lines derived from primary (LM1, LM6, Mel 505) and metastatic (A375M, C8161, WM1158, WM164, WM1361) melanoma lesions. (f) Western blot analysis of GJB5 protein expression in four $BRAF^{V600E}$ melanoma cell lines (WM1158, WM793, WM278, A375M) compared with three $BRAF^{WT}$ melanoma cell lines (Mel 505, HBL, LM6). In (e) and (f) GAPDH was used as a loading control and relative expression signals were calculated and plotted on the right-side graph. Western blots were run more than three times and the analysis summarizes the average signals of all the blots. (g) Protein expression analysis of different connexins on overexpression of GJB5 in $BRAF^{V600E}$ melanoma cells (A375M). Cells were transiently transfected with GJB5 plasmid for 24–48 h and harvested for Western blotting. (h) Protein expression analysis of different connexins on silencing GJB5 in $BRAF^{WT}$ melanoma cells (LM1 and Mel 505). Cells were transfected with small interfering (siRNA) pool mix for GJB5 or with an siRNA scramble control for 24–48 h and harvested for Western blotting. GAPDH was used as a loading control. GAPDH, glyceraldehyde-3-phosphate dehydrogenase.

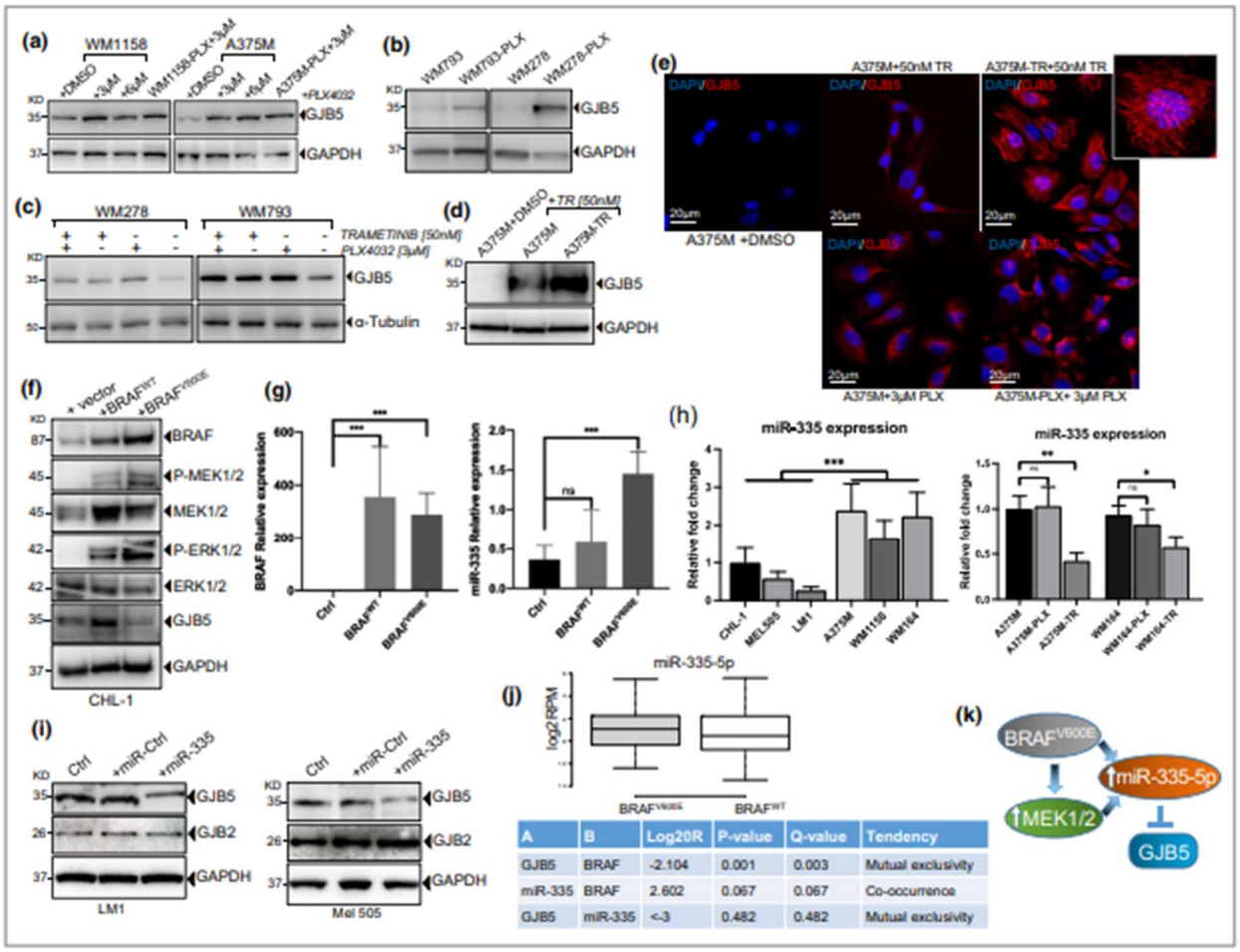

A	B	Log20R	P-value	Q-value	Tendency
GJB5	BRAF	-2.104	0.001	0.003	Mutual exclusivity
miR-335	BRAF	2.602	0.067	0.067	Co-occurrence
GJB5	miR-335	<-3	0.482	0.482	Mutual exclusivity

Figure 4 (a–c). Western blot analysis of GJB5 protein expression. GJB5 expression in $BRAF^{V600E}$ parental melanoma cell lines (WM1158, A375M, WM793, WM278), compared with vemurafenib-resistant melanoma cell lines (WM1158-PLX, A375M-PLX, WM793-PLX, WM278-PLX) treated or not with vemurafenib (PLX4032) and/or trametinib. GAPDH or α-Tubulin were detected as a loading control. (d) Western blot and (e) immunofluorescence staining of A375M cells treated with trametinib or vemurafenib (PLX) and compared with trametinib-resistant or PLX-resistant A375M cells. White scale bars represent 20 μm. (f) Western blot analysis of GJB5 and MAPK protein expression in CHL-1 melanoma cells transiently expressing $BRAF^{WT}$ or $BRAF^{V600E}$. GAPDH was used as a loading control. (g) RT-qPCR of BRAF (left panel) and miR-335-5p expression (right panel) in CHL-1 cells transiently expressing $BRAF^{WT}$ or $BRAF^{V600E}$. (h) RT-qPCR analysis of miR-335-5p in $BRAF^{WT}$ vs. $BRAF^{V600E}$ melanoma cells (left panel) and in $BRAF^{V600E}$ melanoma cells before and after development of BRAF or MEK inhibitor resistance (right panel). (i) Western blot analysis of GJB2 and GJB5 expression on transfection with miR-335 mimics. Cells were transfected for 24–48 h and harvested for Western blotting. GAPDH was used as a loading control. (j) miR-335-5p expression in $BRAF^{mut}$ and $BRAF^{WT}$ samples from the TCGA_SKCM dataset. (Lower panel) Relationship between GJB5 expression, BRAF mutation status and miR-335-5p gain from TCGA_SKCM dataset. (k) Cartoon summarizing how MAPK signalling can regulate GJB5 expression via miR-335-5p in melanoma cells. GAPDH, glyceraldehyde-3-phosphate dehydrogenase; RT-qPCR, reverse-transcriptase quantitative polymerase chain reaction.

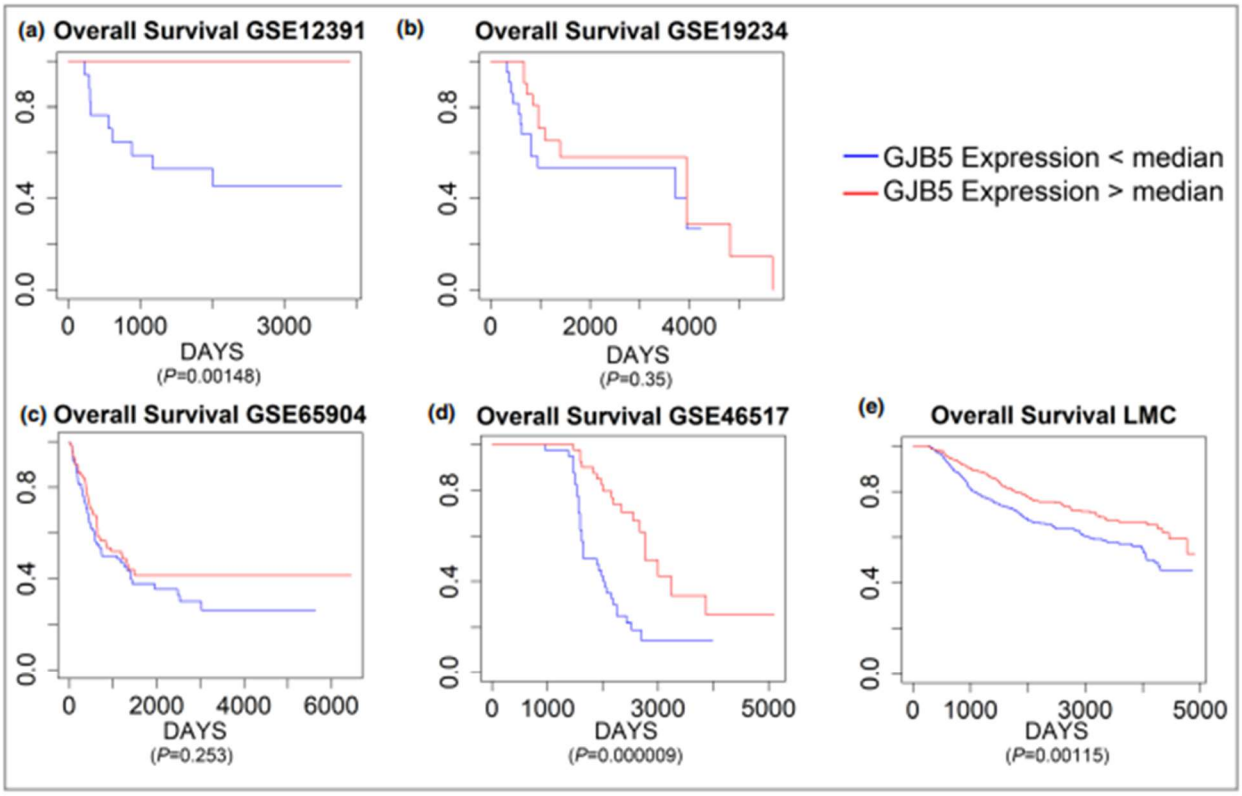

Figure 5 Kaplan–Meier overall survival analysis. Kaplan–Meier overall survival curves in our cohort (a), in GSE19234 (b), GSE65904 (c), GSE46517 (d) and in the Leeds Melanoma Cohort (LMC) (e) datasets. Patients are divided according to GJB5 expression: above the median (red curve) or below the median (blue curve).